ACS Catalysis

Research Article

pubs.acs.org/acscatalysis

Steady-State and Transient Kinetic Studies of the Acetoxylation of Toluene over Pd−Sb/TiO_2

Sven Reining, Evgenii V. Kondratenko,* Narayana V. Kalevaru, and Andreas Martin

Leibniz-Institut für Katalyse e.V., Albert-Einstein-Strasse 29a, 18059 Rostock, Germany

Supporting Information

ABSTRACT: A combination of steady-state catalytic tests, transient studies with isotopic tracers, and kinetic modeling was used to derive detailed insights into the individual reaction pathways in the course of toluene acetoxylation over a Pd−Sb/TiO_2 catalyst. This reaction can be considered as an environmentally friendly route for the production of benzyl alcohol. Benzyl acetate and benzaldehyde are the only products formed from toluene, while acetic acid gives CO_2 in addition to benzyl acetate. The Arrhenius plots revealed apparent activation energies for formation of benzyl acetate and benzaldehyde of 24.9 and 27.5 kJ mol^{-1}, respectively, thus, indicating that these products originate from the same surface intermediate, i.e. benzyl cation. The corresponding value for CO_2 formation was 152.9 kJ mol^{-1}. Transient isotopic studies and their kinetic evaluation demonstrated the participation of lattice oxygen and adsorbed oxygen species in activation of acetic acid, with the latter species favoring oxidation of the acid to CO_2.

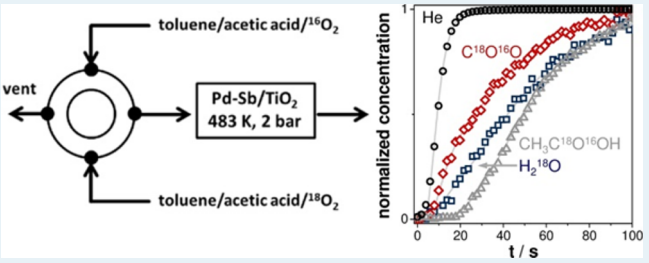

KEYWORDS: *acetoxylation, toluene, SSITKA, oxygen isotopic exchange, transient kinetics, Pd*

1. INTRODUCTION

Alcohols are an important class of compounds in the chemical industry, in particular, with benzyl alcohol being the most industrially key aromatic alcohol.[1] It is used as solvent for surface-coating materials and resins as well as in the manufacturing of perfumes and flavors.[1,2] The global market for the two latter product classes was approximately $6.3 billion in 2006.[3] Its average annual growth rate is estimated to be 4.1% during the years 2014−2019.[4] Benzyl alcohol is mainly produced through hydrolysis of the harmful intermediate benzyl chloride.[5] From an environmental viewpoint, this process is not ecofriendly, because HCl is formed as a side product and additionally chlorine is used to produce benzyl chloride.

The synthesis of benzyl acetate via acetoxylation of toluene followed by subsequent hydrolysis can be considered as a "green and clean" alternative route for the production of benzyl alcohol.[6,7] Our group has intensively investigated acetoxylation of toluene over supported Pd-containing catalysts with the purpose of optimizing their composition[8,9] and reaction conditions.[3] The major drawback of such materials is their on-stream behavior, i.e. there is an activation phase followed by a stable operation for a few hours and then deactivation caused by coke deposition.[10,11] A relatively high long-term stability could, however, be achieved using Cu as a promoter for Pd due to the formation of a core−shell structure with a Pd core and a CuO shell. The activation period was unfortunately established to be too long, i.e. around 60 h.[12,13] The best compromise in terms of on-stream performance is a Pd−Sb/TiO_2 catalyst, which needs an activation time of around 6 h followed by approximately 20 h stable operation.[3] The effect of Sb on the catalytic performance has already been thoroughly investigated in our previous studies.[8,12−14] It was demonstrated that the majority of Sb remains on the surface of TiO_2 as a pentavalent oxide, whereas a small part of Sb is incorporated into Pd particles (as zerovalent Sb) under reaction conditions. In fact, Sb incorporation promotes growth of Pd particles. Formation of large Pd particles (50−100 nm) during the course of the reaction is necessary for enhancing catalytic performance. Despite the positive effect of Sb on catalyst stability, the performance is, still, not sufficient for possible industrial applications. In order to improve catalyst stability or to develop novel long-term stable catalysts, it is highly important to understand mechanistic aspects of catalyst functioning.[15] To the best of our knowledge, no mechanistic studies of toluene acetoxylation were reported up to now. Several contributions, however, dealt with the mechanism of ethylene acetoxylation to vinyl acetate over supported Pd−Au catalysts,[16−25] which is an important chemical intermediate used as reactant for polymerization reactions.[26] After the pioneering work of Samanos et al.,[16] it is in general accepted that the reaction proceeds via a ß-hydride elimination step. As the main side product, CO_2 is formed by combustion of ethylene in the absence and the presence of acetic acid in a temperature range of 413−453 K.

The present contribution was aimed to systematically elucidate possible reaction pathways leading to selective and

Received: March 3, 2016
Revised: June 2, 2016

DOI: 10.1021/acscatal.6b00646
ACS Catal. 2016, 6, 4621−4629

nonselective products in the course of toluene acetoxylation and to determine the nature of oxygen species participating in these processes. In order to complete the mechanistic picture, we combined both steady-state catalytic tests and transient experiments with isotopic tracers, i.e. steady-state isotopic transient kinetic analysis (SSITKA) and switch experiments with selected feed components. Primary and secondary transformations of feed components and reaction products as well as the rate-limiting step(s) were derived from steady-state catalytic tests. Surface precursors and their lifetime were accessed from SSITKA experiments including their kinetic evaluation. Oxygen isotopic exchange measurements provided information about (i) the kind (reversible vs irreversible (non)dissociative adsorption) of interaction of gas-phase O_2 with Pd−Sb/TiO_2 and (ii) nature of active surface oxygen species. On the basis of the results obtained, a detailed mechanistic scheme was developed, and some key aspects for an optimal reactor operation are suggested.

2. EXPERIMENTAL SECTION

2.1. Catalyst Preparation. The acetoxylation catalyst with a nominal composition of 10 wt % Pd-16 wt % Sb/TiO_2 was prepared in two steps according to the procedure previously described in ref 3. To be brief, Sb_2O_3 was initially deposited from aqueous slurry onto the TiO_2 support followed by calcination in air at 673 K for 3 h. Hereafter, the calcined catalyst precursor was further impregnated with a solution of $PdCl_2$ in diluted HCl at 343 K followed by removal of excess H_2O by simple heating of the wet solid at around 423 K. The obtained dry powder material was then calcined at 873 K in a He flow for 4 h. The concentrations of Pd and Sb determined by inductively coupled plasma optical emission spectrometry in the calcined catalyst were 9.6 and 12.5 wt %, respectively. The loss of Sb is probably due to partial formation of volatile $SbCl_3$ upon catalyst calcination in He. The amount of Pd remained practically constant during the preparation procedure.

2.2. Steady-State Catalytic Tests. Steady-state catalytic experiments were performed in a tubular fixed-bed quartz reactor with an internal diameter of 6 mm. A toluene/acetic acid/O_2/(Ne+CH_4) = 1/4/3/17 reaction feed was used in all catalytic tests at a total pressure of 2 bar and four reaction temperatures, i.e. 443, 463, 483, and 503 K. Thereby, CH_4 (5 mol % in Ne) was used as internal standard. The total molar flow was adjusted to 100 mmol h^{-1}, and the amount of catalyst (particles of 400−600 μm) was varied between 0.1 and 0.6 g to achieve different modified residence times and, thus, different degrees of conversion of feed components. The catalyst was diluted with corundum particles in a weight ratio of 3. The toluene/acetic acid mixture and the gaseous feed components were used without any further purification and dosed by HPLC-pump (Shimadzu LC-10Ai) and by mass flow controllers (Bronkhorst), respectively. Before entering the reactor, the liquid reactants were vaporized and mixed with the gaseous compounds statically, i.e. by provoking turbulence in the gaseous stream. The feed components and the reaction products were quantified by an online gas chromatograph (Shimadzu GC 2010) equipped with a thermal conductivity detector (to analyze permanent gases) and a flame ionization detector (to analyze hydrocarbons and oxygenates). Prior to all measurements, a fresh catalyst sample was activated at 483 K for 6 h under continuous flow conditions in the reactant feed mixture mentioned above. A modified residence time of 24 $kg_{catalyst}$ s mol^{-1}_{feed} was adjusted for this activation. The conversion (X) of feed components and product selectivity (S) were calculated using eqs 1 and 2 respectively

$$X = 1 - \frac{x_{i,out}}{x_{i,in}} \tag{1}$$

$$S_{p,i} = \frac{x_{p,out}}{x_{i,in} - x_{i,out}} \tag{2}$$

where x_i and x_p stand for mole fractions of feed components and reaction products, respectively. Subscripts *in* and *out* are used to distinguish between the inlet and outlet fractions.

The absence of external mass-transfer limitations was proven by performing catalytic tests at different total flows but constant modified residence time as suggested in ref 27. The absence of mass-transfer limitations inside pores of catalyst particles was checked experimentally as well. To this end, catalytic tests were performed with catalyst particles of different sieve fractions, while the ratio of catalyst amount to total flow was held constant.[27] Importantly, all these experiments were carried out at 503 K, i.e. the highest reaction temperature applied in the present study. As a result, catalytic tests at lower reaction temperatures are also free of mass-transfer limitations. Additionally, the absence of mass and heat-transfer limitations was proven by theoretical calculations according to Mears, Weisz, and Prater (Table S1).[28,29]

2.3. Catalytic Tests under Transient Conditions. Various transient experiments were carried out in an in-house developed setup at 2 bar and 483 K. This setup is equipped with an online quadrupole mass spectrometer (Balzers Omni Star) and an online gas chromatograph (Agilent 7890 equipped with TCD and FID) to analyze gas-phase components with second and minute resolution, respectively. The mass spectrometer was also applied to distinguish between isotopically labeled compounds. A tubular fixed-bed quartz reactor with an internal diameter of 6 mm was employed. The gaseous components were dosed by mass flow controllers (Brooks). The liquid reactants (toluene and acetic acid) were dosed separately by two HPLC-pumps (Shimadzu), vaporized, and afterward mixed with the gaseous feed. A 4-way valve with pneumatic drive was applied for switching between different feed mixtures within a time, which was significantly shorter than the response of the catalytic system. Prior to all experiments described below in detail, the catalyst was activated according to the same procedure mentioned in the Experimental Section describing steady-state catalytic tests (section 2.2). The absence of mass-transfer effects in the transient experiments has been proven by theoretical calculations as suggested in ref 30. Those authors also showed that heat-transfer limitations in transient experiments can be neglected if their absence is already proven for steady-state catalytic tests.

The measured mass spectroscopic signals were treated mathematically to get values between zero and one as shown in eq 3

$$F(t) = \frac{I(t) - I(0)}{I(\infty) - I(0)} \tag{3}$$

where $F(t)$ is the transient response of a compound, whereas $I(t)$, $I(0)$, and $I(\infty)$ are the transient mass spectroscopic signal, the corresponding signal under steady-state conditions before switching the valve, and the signal under the new steady-state achieved after the switching, respectively.

DOI: 10.1021/acscatal.6b00646
ACS Catal. 2016, 6, 4621−4629

2.3.1. Steady-State Isotopic Transient Kinetic Analysis (SSITKA). For SSITKA experiments, a quartz reactor was filled with 0.4 g of catalyst (200−400 μm) diluted by the 3-fold amount of corundum particles. Toluene/acetic acid/$^{16}O_2$/Ar/He = 1/4/3/3/14 and toluene/acetic acid/$^{18}O_2$/He = 1/4/3/17 mixtures were used as reaction feeds. A modified residence time was adjusted to 24 kg s mol^{-1}. Ar was used for taking the gas-phase hold-up into account, whereas He was an inert standard. After reaching the steady-state with the nonlabeled feed, a switch to the mixture containing labeled $^{18}O_2$ was carried out. A similar SSITKA experiment was performed with 0.2 g of catalyst without the previous activation procedure and using $^{16}O_2$/Ar/He = 5/5/91 and $^{18}O_2$/He = 5/96 mixtures.

The SSITKA experiments were performed under non-differential reactor conditions, and, thus, we have taken into account the concentration profiles along the catalyst bed. Consequently, we applied a reactor model similar to refs 31 and 32 to evaluate the SSITKA tests with toluene/acetic acid/O_2 kinetically (see eqs 4 and 5)

$$\frac{\partial c_i}{\partial t} = -\frac{1}{\tau}\frac{\partial c_i}{\partial x} + \frac{1}{\tau Bo}\frac{\partial^2 c_i}{\partial x^2} + \frac{\rho_b}{\varepsilon_b}\sum_j \nu_{ij} r_j \tag{4}$$

$$\frac{\partial \theta_{i,s}}{\partial t} = \sum_j \nu_{ij} r_j \tag{5}$$

where τ represents the hydrodynamic residence time in s, Bo is the dimensionless Bodenstein number ($Bo = uLD_{ax}^{-1}$), ρ_b is the density of the catalyst bed in kg m^{-3}, ε_b is the void fraction of the catalyst bed (dimensionless), x is the axial position in the catalyst bed (dimensionless), t is the time in s, c_i is the concentration of component i in mol m^{-3}, and $\Theta_{i,s}$ is the surface concentration of the intermediate i in mol kg_{cat}^{-1}. Thereby, the void fraction was set to 0.45, and the density of the catalyst bed was determined using a graduated cylinder and set to 2000 kg m^{-3}. The following initial and boundary conditions were used to solve the system of (partial) differential equations.

The following equations show the initial conditions (eq 6) and boundary conditions for products (eq 7) and $^{18}O_2$ (eq 8)

$$c_i(t=0) = 0; \quad \theta_i(t=0) = 0 \tag{6}$$

$$\left.\frac{\partial^2 c_i}{\partial x^2}\right|_{x=1} = 0; \quad c_i|_{x=0} = 0 \tag{7}$$

$$c_i|_{x=0} = 6 - \exp(-10t) \tag{8}$$

An input function was used as boundary condition for $^{18}O_2$ due to the numerical difficulties applying a Heaviside function, i.e. an ideal step input. Thereby, the molar concentration of 6 mol m^{-3} was used as input for $^{18}O_2$, which is equivalent to the oxygen partial pressure of 0.24 bar adjusted in the experiment. To solve the system of (partial) differential equations, a suitable procedure for evaluation of transient kinetic data using the PDEPE routine as suggested in ref 33 was adopted. This algorithm enables solving partial differential equations in one space dimension. Thereby, the numerical method of lines is used, which reduces the system of partial differential equations to a system of ordinary differential equations by discretization in axial direction.[34,35] Due to the different time scales of the numerical solution and the experimental data, the obtained solution was interpolated to get the concentrations corresponding to the time scale of the experimental data. Afterward, the Levenberg−Marquardt-algorithm was applied to fit the model to the experimental data using the sum of least-squares as objective function.[36,37]

Reasonable starting values were determined as follows: first of all, the experimental data for each component were fit respectively to models, which were as simple as possible until a satisfying description was reached. These different models represent various adsorbate precursors leading to gas-phase reaction products, i.e. single pool, two pools in series, and two pools in parallel and one pool in series to the prior parallel pools, respectively. The obtained rate constants for the models describing the transients of the single components were used as starting values for the overall model.

2.3.2. Transient Response Method. Quartz reactor was filled with 0.2 g of catalyst diluted by the 3-fold amount of corundum particles. A modified residence time of 8 kg s mol^{-1} was adjusted. After the activation procedure of 6 h, the catalyst was heated at atmospheric pressure in a flow (30 mL min^{-1} in total) of 5 mol % CH_4 in Ne up to 523 K for 15 min to clean its surface from adsorbates formed during the activation procedure. Hereafter, the reactor was cooled to 483 K with a simultaneous increase in pressure to 2 bar followed by switching to the toluene/acetic acid/O_2/Ar = 1/4/3/17 reaction mixture. An additional experiment was performed, in which we switched between toluene/acetic acid/O_2/Ar = 1/4/3/17 and toluene/acetic acid/(CH_4+Ne) = 1/4/20 reaction feeds.

3. RESULTS AND DISCUSSION

3.1. Overall Reaction Pathways in Toluene Acetoxylation. For deriving insights into overall reaction pathways of product formation in the course of toluene acetoxylation, steady-state catalytic tests were performed at different contact times to achieve different degrees of conversion of feed components; the longer the contact time, the higher the conversion was observed as expected. The purpose of these tests was to investigate the effect of conversion on the selectivity to gas-phase products, which were benzyl acetate, benzaldehyde, and carbon dioxide. The selectivity was calculated from the corresponding yields and the conversion of either toluene or acetic acid according to eqs 1 and 2. Such calculations enable to check if some other not-detected products (for example surface deposits) were also formed from feed components.

We shall begin with the discussion of product selectivity calculated with respect to toluene. It is important to highlight that irrespective of toluene conversion an overall selectivity to benzyl acetate and benzaldehyde (both products are definitively formed from toluene) was around 100%. This strongly suggests that carbon dioxide is practically not formed from toluene and/or the above reaction products. It should probably originate from acetic acid (see below). Therefore, the selectivity to CO_2 was not used for analyzing the selectivity-conversion plot on toluene basis in Figure 1a. In a broad conversion range, the selectivity to benzyl acetate was well above 90% and only slightly decreased with an increase in the conversion. Since the selectivity to benzaldehyde increased accordingly, it can be concluded that benzyl acetate primarily formed from toluene was further converted to benzaldehyde to a small extent. The latter product should also be formed directly from toluene otherwise its selectivity would be zero when toluene conversion

DOI: 10.1021/acscatal.6b00646
ACS Catal. 2016, 6, 4621−4629

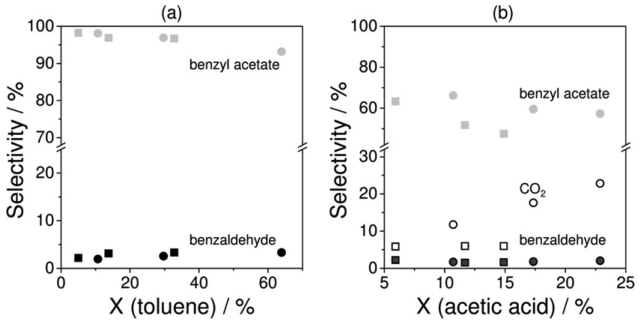

Figure 1. Selectivity-conversion plots on the basis of toluene (a) and acetic acid (b) at 483 K (squares) and 503 K (circles).

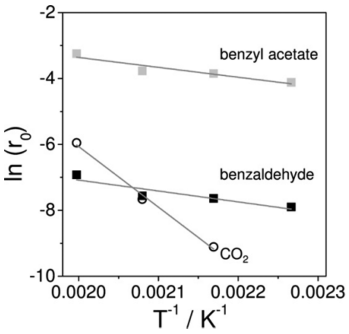

Figure 2. Arrhenius plot of the rates of formation of main gas-phase reaction products.

is approaching zero. This direct pathway plays, however, a minor role in the course of toluene acetoxylation.

Figure 1b shows the selectivity-conversion plot obtained on acetic acid basis. It is obvious that overall product selectivity is well below 100%, which gives indications that another product(s) must be formed from acetic acid. Since no additional gas-phase components were detected by our online GC analysis, we suggest that acetic acid might be converted to carbon deposits and/or CO_2; conversion of toluene and/or benzyl acetate to these products can be excluded when bearing in mind the results shown in Figure 1a. CO_2 selectivity did not change with rising conversion of acetic acid at 483 K. From a mechanistic viewpoint, we put forward that acetic acid is decomposed to gas-phase CO_2 and surface carbon-containing species in agreement with previous studies.[19,38−41] The latter species can be further oxidized to CO_2 as concluded from the fact that CO_2 selectivity at 503 K increased with an increase in acetic acid conversion.

In summary, different reaction pathways of toluene and acetic acid transformations in the course of toluene acetoxylation were identified from the analysis of the dependence of product selectivity on conversion of individual feed components. Toluene is mainly converted to benzyl acetate and to a minor extent to benzaldehyde. In addition to the desired acetoxylation, acetic acid decomposition to CO_2 and surface carbonaceous species also occurs to a certain extent.

To derive further kinetic insights into toluene acetoxylation, we performed additional steady-state tests at different reaction temperatures. The idea behind these tests was to determine apparent activation energies (E_a) of formation of benzyl acetate, benzaldehyde, and carbon dioxide and to check whether these products are formed from the same intermediate. Since the tests were performed under integral conditions, we treated all experimental data according to the below procedure to calculate initial differential reaction rates. The yield of each reaction product was plotted as a function of modified residence time (τ). Afterward, these data were fitted by a polynomial function of second order (in the case of benzyl acetate) and linearly (benzaldehyde and CO_2). The derivative of the respective function was calculated at $\tau = 0$ to obtain the initial reaction rate. This procedure was performed for different temperatures. The obtained Arrhenius plots for each product are given in Figure 2. The E_a value determined for benzyl acetate was around 24.9 ± 6.1 kJ·mol^{-1} and did not significantly differ from the value of 27.5 ± 7.8 kJ·mol^{-1} for benzaldehyde. This result strongly suggests that these products are formed with the same rate-limiting step. As will be demonstrated below, the slow step is the activation of adsorbed toluene to form a benzyl cation, which can react with either surface acetate or the surface hydroxyl-group to yield benzyl acetate and benzaldehyde, respectively. CO_2 should be formed from another intermediate as concluded from the significantly higher E_a value of 152.9 ± 10.9 kJ·mol^{-1}. Further mechanistic insights into CO_2 formation were derived from transient experiments described and thoroughly discussed in the sections below.

3.2. Transient Experiments: Mechanistic Insights into Individual Reaction Pathways. The so-called transient response method was used to further elucidate the reaction mechanism.[42−44] In this way, we switched from an inert flow to a reactive flow containing toluene, acetic acid, and oxygen and monitored transient responses of feed components and reaction products by means of an online MS. Such time-resolved analyses enable the investigation of desired and side reactions under different coverages by surface species, i.e. from a clean catalyst surface to that with steady-state concentration of surface intermediates. As described in the Experimental Section, the transient responses of feed components and reaction products were normalized with respect to the corresponding steady-state concentrations (see eq 3). The normalized concentration of zero represents the steady-state under inert flow, and one is related to the new steady-state under the reaction feed.

Figure 3 illustrates the obtained transients before and after switching. Obviously, the normalized CO_2 and H_2O concentrations strongly increase within the first 10 s in the reaction feed and then decrease to approach the steady-state values after 50 s on stream. The concentration of toluene also passes a maximum, which is, however, significantly less pronounced

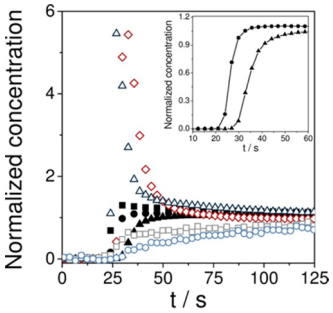

Figure 3. Transient responses after a step input of the toluene/acetic acid/O_2/Ar = 1/4/3/17 reaction feed. Reactants: toluene (■), acetic acid (▲), O_2 (●); products: H_2O (◇, red), CO_2 (Δ, dark blue), benzyl acetate (○, light blue), benzaldehyde (□, gray), T = 483 K, p = 2 bar.

DOI: 10.1021/acscatal.6b00646
ACS Catal. 2016, 6, 4621−4629

than for CO_2 and H_2O. For all other reaction products and feed components, their concentration increased continuously from zero to the steady-state value without passing a maximum with rising reaction time.

It is worth mentioning that the transient of acetic acid is delayed by approximately 10 s with respect to oxygen (see the insert in Figure 3) and toluene. This indicates that toluene was stable, while acetic acid was completely consumed within this period of time, where the formation of CO_2 and H_2O reached the maximal values. In agreement with the results of steady-state tests in Figure 1, the results shown in Figure 3 further support that acetic acid undergoes decarboxylation to CO_2 and H_2O on the clean catalyst surface. This conclusion is also supported by previous DFT calculations of the mechanism of acetic acid decomposition on Pd(111).[38] Surface acetate was predicted to form upon interaction of gas-phase acetic acid with free Pd surface sites. This intermediate turns in parallel to the surface via a free Pd^0 site followed by decomposition to CO_2, H_2O, and coke species.[19,38,39] The experimental results from the present study suggest that this undesired reaction pathways is hindered in the presence of adsorbates formed from acetic acid and/or toluene.

We now discuss the responses of benzaldehyde and benzyl acetate. One can see that the concentration of the former product increased steeply in comparison with that of benzyl acetate. Such difference in the temporal evolution of these transients can be understood as follows. Since acetic acid was decarboxylated to CO_2 and H_2O within the first seconds on stream, its surface coverage was low, and, thus, the formation of benzyl acetate was hindered. Contrarily, high water concentration during this period of time should favor formation of hydroxyl groups, which can react with the benzyl cation formed from toluene to yield benzyl alcohol. This alcohol can be easily oxidized to benzaldehyde as proven in separate experiments on benzyl alcohol oxidation at 483 K using benzyl alcohol/acetic acid/O_2/inert = 1/4/3/17 feed mixture (Figure S1). Benzyl alcohol was nearly fully converted with a high selectivity to benzaldehyde of around 95%. In spite of the presence of acetic acid, only small amounts of benzyl acetate were formed (Figure S1). In the same way, separate experiments were carried out using benzaldehyde as feed component instead of toluene. No conversion could be obtained that is in accordance with the selectivity-conversion plot shown in Figure 1 (a).

Further mechanistic insights can be obtained from the analysis of the responses at higher reaction times, i.e. higher coverage of the catalyst surface. In contrast to the response of CO_2, the response of H_2O passed through a minimum (see Figure S2). After passing the minimum at around 125 s (Figure 3), the H_2O response increased in the same way as the response of the target product benzyl acetate. This indicates two different reaction pathways of H_2O formation. At low surface coverage, H_2O is formed through the oxidative decomposition of acetic acid as discussed above. After passing the minimum in H_2O concentration, the decomposition is hindered because the surface becomes covered by adsorbates formed from acetic acid and toluene. Therefore, the formation of benzyl acetate dominates, and H_2O is mainly formed through the target reaction. Thereby, the latter rate of H_2O formation is much slower in comparison to the first reaction pathway of H_2O formation from acetic acid at low surface coverages.

For clarifying the role of lattice oxygen in the acetoxylation of toluene, an additional transient experiment was performed, in which O_2 was removed from the standard toluene acetoxylation feed and then again cofed after a certain period of time. This sequence was repeated two times. The total pressure and partial pressures of acetic acid and toluene were kept constant. Figure 4 shows the normalized concentrations of CO_2, H_2O, and O_2 in

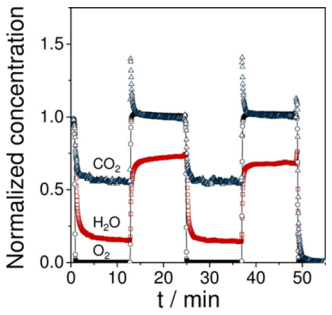

Figure 4. Transient responses of CO_2, H_2O, and O_2 after switching from the toluene/acetic acid/O_2/Ar = 1/4/3/17 reaction mixture to a flow of 5 mol % CH_4 in Ne at 483 K and 2 bar.

the absence and the presence of the latter in the standard toluene acetoxylation feed. They were normalized with respect to the values obtained under steady-state reaction conditions in the presence of all reactants. In comparison with CO_2 and H_2O, the concentration of O_2 sharply decreases or increases upon removal of O_2 from the reaction feed or by cofeeding of O_2, thus indicating that gas-phase O_2 weakly interacts with the catalyst. It is important to note that all reaction products including benzyl acetate and benzaldehyde were formed in the absence of gas-phase O_2 but in lower amounts.

CO_2 was formed by decarboxylation of acetic acid as already explained above. An overshoot in the CO_2 transients was observed again (Figure 3), but the formation pathways of CO_2 must be different in this case due to an increased coverage by various surface intermediates. We assume an oxidation of surface coke species as a reason for the overshoot in the CO_2 formation. Interestingly, no overshoot in the H_2O response was observed, which is in contrast to Figure 3. The reason is the difference in the reaction pathways of H_2O formation. In this case, H_2O is mainly formed as byproduct in the synthesis of benzyl acetate, because the surface is covered by the reactants in contrast to the results shown in Figure 3 where the surface was free of adsorbates before switching to a reactive feed. Thus, H_2O was mainly formed by complete oxidation of acetic acid which cannot take place in the absence of gas-phase O_2 so that only the decarboxylation can occur and hence a CH_x group remains on the surface. The responses of benzyl acetate and benzaldehyde further underline this conclusion because both showed similar characteristics as the response of H_2O did (not shown here).

The formation of H_2O even in the absence of gas-phase O_2 can be explained by the participation of lattice oxygen. Hydrogen abstracted from toluene forms a Pd−H species which can be removed from the surface by remaining hydroxyl groups that contain lattice oxygen. The reoxidation of the catalyst is not possible anymore due to the missing gas-phase O_2 which in turn resulted in an exponential decrease in the rate of H_2O formation.

3.3. Steady-State Isotopic Transient Kinetic Analysis.

To get insights into the kind (reversible vs irreversible) of interaction of O_2 with the Pd−Sb/TiO_2 catalyst, we also investigated oxygen isotopic exchange over fresh or activated

DOI: 10.1021/acscatal.6b00646
ACS Catal. 2016, 6, 4621−4629

catalyst samples. Irrespective of the catalyst state, $^{16}O^{18}O$ was not observed and the responses of $^{16}O_2$ and $^{18}O_2$ were very similar to the response of the inert tracers and overlaid with them (see Figure 5). Thus, gas-phase O_2 was concluded to

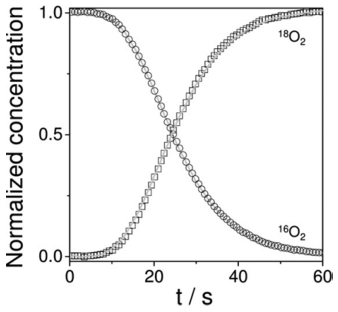

Figure 5. Transient responses of oxygen (open symbols) and helium (solid lines) after switching from $^{16}O_2$/Ar/He to $^{18}O_2$/He over the activated Pd−Sb/TiO_2 catalyst at 483 K.

interact with the catalyst weakly and adsorbed irreversibly. A similar result was obtained for O_2 activation on the Pd/Cd/silica/K catalyst used in the acetoxylation of ethylene.[24]

For analyzing a possible role of lattice and adsorbed oxygen species in CO_2 and H_2O formation as well as in transformation of acetic acid, a SSITKA experiment was performed. In this case, Pd−Sb/TiO_2 was treated at 483 K in toluene/acetic acid/$^{16}O_2$/Ar/He = 1/4/3/3/14 until steady-state operation was achieved. Hereafter, this feed was replaced by a toluene/acetic acid/$^{18}O_2$/He = 1/4/3/17 feed for approximately 15 min followed by switching back to the reaction feed without isotopically labeled oxygen (Figure 6). No formation of $^{16}O^{18}O$ was observed, which is in good agreement with the results discussed above in the context of Figure 5. These results also indicate that both feed components and reaction products do not affect the mechanism of oxygen activation.

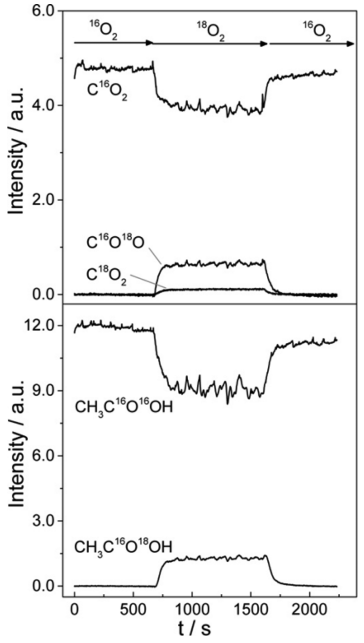

Figure 6. Transient responses of labeled and nonlabeled carbon dioxide and acetic acid obtained from the SSITKA experiment at 483 K and 2 bar (for details see section 2.3.1).

Three differently labeled carbon dioxide species were observed: $C^{16}O_2$, $C^{16}O^{18}O$, and $C^{18}O_2$ with the latter being formed in traces (Figure 6). The transient of $C^{16}O_2$ fell slightly within approximately 10 min on stream after switching to toluene/acetic acid/$^{18}O_2$/He = 1/4/3/17, while those of $C^{16}O^{18}O$ and $C^{18}O_2$ increased. Hereafter, the concentration of all carbon dioxide isotopes did not practically change with rising time-on-stream. $C^{16}O_2$ was always the main isotope. Since $^{16}O_2$ was not present in the reaction feed and Pd−Sb/TiO_2 did not practically exchange its lattice oxygen with gas-phase O_2, the precursor of CO_2 must contain at least one oxygen atom. On the basis of the results of steady-state tests in sections 3.1 and 3.2, acetic acid should be the only precursor in the formation of CO_2. This statement is actually supported by the SSITKA results shown in Figure 6. Similar to $C^{16}O_2$ and $C^{16}O^{18}O$, the amount of $CH_3C^{16}O^{16}OH$ decreases, while the formation of $CH_3C^{16}O^{18}OH$ increases within approximately the first 10 min on stream after switching to toluene/acetic acid/$^{18}O_2$/He = 1/4/3/17 and then their concentrations do not alter much with time-on-stream. From a mechanistic point of view, surface acetate can partially exchange its oxygen followed by reconstitution to acetic acid and desorption into the gas-phase or decomposition to $C^{16}O^{18}O$ and surface carbon species. Previous DFT calculations consider a similar mechanistic concept for the acetate-Pd(111) system.[38]

The SSITKA results were kinetically evaluated to estimate the number of surface intermediates leading to H_2O and CO_2 and their surface residence time as well as to check if different oxygen species are formed from gas-phase O_2. In this context, we initially estimated mass transport parameters (*Bo* and τ in eq 4) from the transient response of He used as an inert tracer in our tests. The *Bo* and τ values were 8.9 and 11.8 s, respectively. The low value of *Bo* can be explained by the dead volume before the reactor. Thus, around 21 s of the measured data directly after switching the valve were not taken into account whereby *Bo* accordingly decreased. Taking the dead volume into account, a *Bo* number of 104 was calculated from the jump in He concentration by the standard procedure known from chemical reaction engineering textbooks.[45−47] For *Bo* numbers larger than 80, plug flow can be assumed.[46] Thus, the applied procedure had no influence on the kinetic parameters.

The rate constant of the adsorption of $^{18}O_2$ (k_{ads}) was determined manually by performing numerical simulations of the reactor model using different values of k_{ads}. This procedure was applied until the experimentally measured O_2 conversion of 14.1% at the reactor outlet was adjusted in the numerical simulation. The conversion of toluene and acetic acid was 40.8% and 16.8%, respectively. Thus, a simplified kinetic evaluation of SSITKA experiments for differential flow reactors[48,49] was not trustworthy. Therefore, an integral reactor model was applied to kinetically evaluate the acetoxylation under such high degrees of conversion. As a first step, we used transient responses of isotopically labeled water, carbon dioxide, and acetic acid to estimate the number of independent surface intermediates (pools), from which respective gas-phase products are formed. The simplest model (one pool) was initially used to describe the experimental data. If this fitting was not satisfied, the model complexity was increased by adding one or several additional pools.

As a result, the model with two pools in series described the transient response of $C^{18}O_2$ correctly. Two pools in parallel and one pool in series to the previous pools were necessary to describe the $C^{18}O^{16}O$ and $H_2{}^{18}O$ responses, and two pools in

DOI: 10.1021/acscatal.6b00646
ACS Catal. 2016, 6, 4621−4629

series could fit the data of labeled acetic acid satisfactorily. The heterogeneity (several pools) of surface intermediates was additionally validated by the below theoretical analysis of the derivative of the experimental responses at $t = 0$. A positive derivative indicates a direct formation of the product from one surface intermediate. A derivative of zero resulting from a consecutive surface reaction means the necessity of a minimum of two pools in series. In our case, the derivatives of the transients at $t = 0$ showed a value of zero for all the labeled compounds. Thus, the necessity of at least two pools in series as mentioned above is confirmed. On the basis of these results, two models using different oxygen species were developed (see Figure 7).

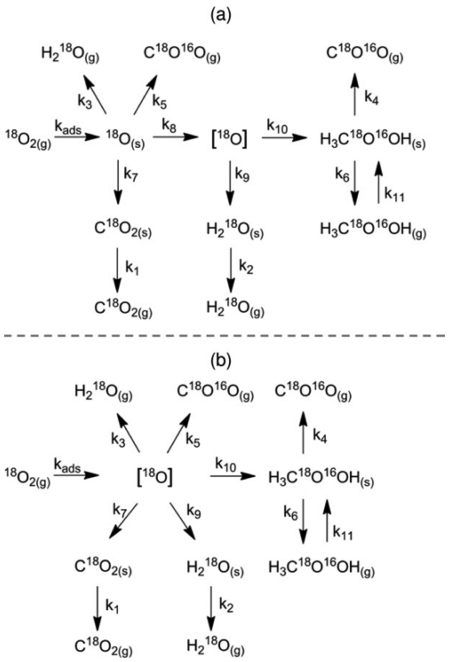

Figure 7. Mechanistic schemes representing individual reaction steps leading to labeled acetoxylation products with participation of two different oxygen species (a) or one oxygen species (b).

The labeled $^{18}O_2$ adsorbs irreversibly on the surface of the catalyst to yield an unselective oxygen species ($^{18}O_s$) which is then inserted into the lattice ([^{18}O]) in a subsequent step. CO_2 and H_2O are formed from the unselective oxygen species as a consequence of acetic acid decomposition. H_2O is also formed from the selective oxygen species as a side product in the formation of the target product benzyl acetate. For the labeled acetic acid, a reversible adsorption step (k_{11}) was assumed because acetic acid is a reactant in the reaction system, and, thus, this assumption is reasonable.

The experimental data for the labeled products CO_2, H_2O, and acetic acid and the respective fits are shown in Figure 8. For the sake of better clarity, the results for $C^{18}O_2$ are not shown in Figure 8, but they are given in the Supporting Information (Figure S3).

The model presented in Figure 7a describes the experimental data of all labeled products well. An F-test as applied in ref 50, for instance, showed on the 95% level that model a) can describe the data significantly better than model b) (see Figure 8b). Consequently, we assume the participation of two oxygen species in the acetoxylation of toluene: an unselective oxygen species, which takes part in the decomposition of acetic acid,

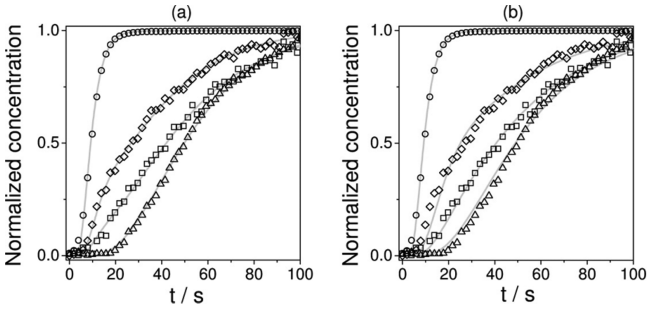

Figure 8. Comparison between normalized experimental responses of He (○), $C^{16}O^{18}O$ (◇), $H_2{}^{18}O$ (□), and $CH_3C^{16}O^{18}OH$ (Δ) and their simulated counterparts calculated under assumption of participation of two different (a) or one (b) oxygen species in formation of water, carbon dioxide, and acetic acid at 483 K and 2 bar.

and one selective oxygen species, which forms the labeled acetic acid as well as H_2O as byproduct of the target reaction, i.e. the formation of benzyl acetate. The respective kinetic parameters determined by data fitting as mentioned in the Experimental Section are given in Table 1.

Table 1. Kinetic Parameters of Individual Reaction Pathways in Figure 7(a) Obtained from Fitting SSITKA Experiments

	rate constant/s^{-1}
k_1	0.0232
k_2	0.0351
k_3	0.0176
k_4	0.0657
k_5	0.336
k_6	0.0028
k_7	0.4
k_8	0.512
k_9	0.0129
k_{10}	0.0578
k_{11}	0.167

The most important point extracted from Table 1 is the fast insertion of oxygen into the Pd lattice (k_8) forming the selective oxygen species. In other words, the surface residence time of the unselective oxygen species is very low. This result obtained from kinetic analysis is in accordance with the high selectivity to benzyl acetate (89.8%) based on toluene conversion measured in the SSITKA experiment and also in separate catalytic tests discussed above (see Figure 1). Furthermore, it is worthwhile to compare the different rate constants of CO_2 formation, i.e. k_1, k_4, k_5, and k_7. The formation of $C^{18}O_2$ and $C^{18}O^{16}O$ from the unselective oxygen species is fast and proceeds with comparable rate constants values (k_5, k_7), but the release from the surface is slow in case of $C^{18}O_2$ (k_1). The big difference of 1 order of magnitude between the rate constants of $C^{18}O^{16}O$ formation (k_4, k_5) confirms the assumption of different reaction pathways. A high activation barrier must be overcome for the formation of $C^{18}O^{16}O$ from labeled surface acetate (k_4). This result is in agreement with the high activation energy of 152.9 kJ mol^{-1} obtained for the formation of nonlabeled CO_2 from acetic acid (see Figure 2). Besides the mentioned aspects, the formation of $H_2{}^{18}O$ from lattice oxygen ([^{18}O]) should be briefly discussed, because this reaction pathway contains a slow step (k_9) compared to other rate constants. As mentioned above, the H-abstraction from toluene is assumed as rate-

DOI: 10.1021/acscatal.6b00646
ACS Catal. 2016, 6, 4621−4629

limiting step; this slow step is also involved in the formation of H_2O due to the removal of the abstracted hydrogen by oxygen. Thus, the kinetic analysis confirms the assumption of the rate-limiting step by the slow rate of H_2O formation (k_9).

3.4. Mechanistic Concept for Tuning Catalyst Performance. On the basis of the present research and our previous studies,[51,52] as well as under consideration of literature data on acetoxylation of lower olefins[19,53] and decomposition/adsorption of acetic acid[38−41] over Pd-containing catalysts, we suggest the following mechanistic concept of acetoxylation of toluene. Metallic Pd and PdO are the two catalytically active sites participating in the activation of the feed components. Both these species coexist within one Pd nanoparticle. Metallic Pd species are responsible for heterolytic splitting of the C−H bond in the methyl group of toluene resulting in adsorbed benzyl cation and hydride species, whereas acetic acid dissociates on PdO sites to yield adsorbed acetate and a proton connected to Pd^{2+} and O^{2-}, respectively. The acetate species mainly reacts with the benzyl cation to the desired benzyl acetate but can also be converted to CO_2, H_2O, and coke precursors via an additional active site, i.e. probably metallic Pd. Another side reaction in the course of toluene acetoxylation is the coupling of benzyl cation with a neighboring hydroxyl group to form benzyl alcohol, which is easily oxidized to benzaldehyde even in the presence of acetic acid (Figure S1). The formed aldehyde is stable against its further conversion to benzyl acetate, CO_2, or carbon deposits. As concluded from the above-described SSITKA experiments, the desired benzyl acetate formation takes place with participation of lattice oxygen species responsible for H_2O generation from hydride and hydroxyl species connected to metallic Pd and Pd^{2+}, respectively. For charge compensation, Pd^{2+} should be reduced to Pd upon the formation of H_2O by taking electrons from the hydride. The Pd^{2+}/Pd redox cycle has been previously suggested for acetoxylation of lower olefins.[53] The detailed mechanism of reoxidation of metallic Pd remains unclear, i.e. whether Pd is oxidized by gas-phase O_2 directly or by lattice oxygen from the cocomponent Sb which is initially oxidized by gas-phase O_2.

Bearing in mind the above mechanistic scheme, the selectivity to benzyl acetate should depend on the rates of benzyl cation reaction with surface acetate (desired reaction pathway) or hydroxyl groups (undesired side reaction). Thus, a high partial pressure of acetic acid should be applied to increase the coverage by the former surface intermediates. As demonstrated in this work, acetic acid is not involved in the rate-limiting step of the desired reaction. Thus, an increased acetic acid/toluene feed ratio leads to a decrease in the conversion of acetic acid. The reduced acetic acid conversion is also a benefit since the formation of CO_2 can be suppressed in this way, and simultaneously the selectivity to the target product benzyl acetate can be increased (cf. Figure 1b). The results from this study clearly explain the enhanced catalytic performance applying higher total pressure as investigated in a previous study.[11] The increase in the concentration of adsorbed toluene leads to an enhanced activity due to its participation in the rate-limiting step, and the higher surface concentration of acetate leads to an enhanced selectivity. Furthermore, an increase in the reaction temperature, e.g. 503 K, seems to be beneficial to increase the yield of the target product. This suggestion can be deduced from the fact that consecutive reactions take place only to a minor extent even at higher reaction temperature.

CONCLUSIONS

The reaction mechanism of the acetoxylation of toluene over the Pd−Sb/TiO_2 catalyst was elucidated, for the first time, by means of steady-state catalytic tests and transient kinetic studies with isotopic tracers. The breaking C−H bond in the methyl group of toluene on Pd^0 sites was found to be the rate limiting step leading to surface benzyl cation. This intermediate reacts with OH or with surface acetate formed from acetic acid to yield benzyl alcohol or the main product benzyl acetate, respectively. The former product is easily oxidized to benzaldehyde. All these products and toluene were established to be stable against oxidation to CO_2, which originates from acetic acid exclusively. The detailed kinetic evaluation of isotopically labeled product responses using numerical simulations suggested that adsorbed oxygen species participate in CO_2 formation, while lattice oxygen is responsible for the formation of surface acetate which reacts further with the benzyl cation to the target benzyl acetate. On the basis of the obtained results, suggestions were deduced for an enhanced reactor operation.

ASSOCIATED CONTENT

Supporting Information

The Supporting Information is available free of charge on the ACS Publications website at DOI: 10.1021/acscatal.6b00646.

Transient responses of CO_2, H_2O, and benzyl acetate at higher times; SSITKA data of $C^{18}O_2$ and the corresponding fits; TPR/TPO cycle of the spent Pd−Sb/TiO_2 catalyst; product distribution while dosing benzyl alcohol instead of toluene in the reaction feed mixture; theoretical calculations of transport limitations (PDF)

AUTHOR INFORMATION

Corresponding Author

*E-mail: evgenii.kondratenko@catalysis.de.

Notes

The authors declare no competing financial interest.

ACKNOWLEDGMENTS

Dedicated to Prof. Angelika Brückner on the occasion of her 60th birthday. Dr. Sergey Sokolov is gratefully acknowledged for performing the TPR/TPO tests.

REFERENCES

(1) Brühne, F.; Wright, E. Benzyl Alcohol. In *Ullmann's Encyclopedia of Industrial Chemistry*; VCH Verlag GmbH & Co. KGaA: Weinheim, 1985; pp 1−8.

(2) Fahlbusch, K.-G.; Hammerschmidt, F.-J.; Panten, J.; Pickenhagen, W.; Schatkowski, D.; Bauer, K.; Garbe, D.; Surburg, H. Flavors and Fragrances. In *Ullmann's Encyclopedia of Industrial Chemistry*; Wiley-VCH Verlag GmbH & Co. KGaA: Weinheim, 2003; pp 73−201.

(3) Madaan, N.; Gatla, S.; Kalevaru, V. N.; Radnik, J.; Lücke, B.; Brückner, A.; Martin, A. *Top. Catal.* **2011**, *54*, 1197−1205.

(4) Growth Opportunities for the Global Flavors and Fragrances Market 2014−2019: Trends, Forecasts and Opportunity Analysis. http://www.researchandmarkets.com/research/q9vlcq/growth (accessed Jan 6, 2016).

(5) Wittcoff, H. A.; Reuben, B. G.; Plotkin, J. S. Chemicals and Polymers from Toluene. In *Industrial Organic Chemicals*; John Wiley & Sons, Inc.: NJ, 2013; pp 375−382.

DOI: 10.1021/acscatal.6b00646
ACS Catal. 2016, 6, 4621−4629

(6) Okada, T.; Hanaya, M.; Hattori, A.; Miyake, T.; Nagira, N.; Ikumi, S.; Hori, T.; Mizui, N. Process for producing benzyl acetate and benzyl alcohol. US Patent 6057482A, May 2, 2000.
(7) Benhmid, A.; Kalevaru, V. N.; Bischoff, S.; Martin, A.; Lücke, B. Festphasenkatalysator, Verfahren zu seiner Herstellung und seine Anwendung zur Herstellung von Arylestern. DE Patent 102004002262A1 Aug. 11, 2004.
(8) Kalevaru, V. N.; Benhmid, A.; Radnik, J.; Pohl, M. M.; Bentrup, U.; Martin, A. *J. Catal.* **2007**, *246*, 399−412.
(9) Gatla, S.; Madaan, N.; Radnik, J.; Kalevaru, V. N.; Lücke, B.; Martin, A.; Bentrup, U.; Brückner, A. *ChemCatChem* **2011**, *3*, 1893−1901.
(10) Madaan, N.; Gatla, S.; Kalevaru, V. N.; Radnik, J.; Lücke, B.; Brückner, A.; Martin, A. *J. Catal.* **2011**, *282*, 103−111.
(11) Madaan, N.; Gatla, S.; Kalevaru, V. N.; Radnik, J.; Pohl, M.-M.; Lücke, B.; Brückner, A.; Martin, A. *ChemCatChem* **2013**, *5*, 185−191.
(12) Radnik, J.; Pohl, M.-M.; Kalevaru, V. N.; Martin, A. *J. Phys. Chem. C* **2007**, *111*, 10166−10169.
(13) Benhmid, A.; Narayana, K. V.; Martin, A.; Lücke, B.; Pohl, M.-M. *Chem. Lett.* **2004**, *33*, 1238−1239.
(14) Gatla, S.; Radnik, J.; Madaan, N.; Pohl, M.-M.; Mathon, O.; Rogalev, A.; Narayana Kalevaru, V.; Martin, A.; Pascarelli, S.; Brückner, A. *Chem. - Eur. J.* **2015**, *21*, 15280−15289.
(15) Kondratenko, E. V. *Top. Catal.* **2013**, *56*, 858−866.
(16) Samanos, B.; Boutry, P.; Montarnal, R. *J. Catal.* **1971**, *23*, 19−30.
(17) Nakamura, S.; Yasui, T. *J. Catal.* **1970**, *17*, 366−374.
(18) Gao, F.; Wang, Y.; Calaza, F.; Stacchiola, D.; Tysoe, W. T. *J. Mol. Catal. A: Chem.* **2008**, *281*, 14−23.
(19) Neurock, M.; Provine, W. D.; Dixon, D. A.; Coulston, G. W.; Lerou, J. J.; van Santen, R. A. *Chem. Eng. Sci.* **1996**, *51*, 1691−1699.
(20) Stacchiola, D.; Calaza, F.; Burkholder, L.; Schwabacher, A. W.; Neurock, M.; Tysoe, W. T. *Angew. Chem., Int. Ed.* **2005**, *44*, 4572−4574.
(21) Plata, J. J.; García-Mota, M.; Braga, A. A. C.; López, N.; Maseras, F. *J. Phys. Chem. A* **2009**, *113*, 11758−11762.
(22) Han, Y. F.; Wang, J. H.; Kumar, D.; Yan, Z.; Goodman, D. W. *J. Catal.* **2005**, *232*, 467−475.
(23) Han, Y. F.; Kumar, D.; Goodman, D. W. *J. Catal.* **2005**, *230*, 353−358.
(24) Crathorne, E. A.; Macgowan, D.; Morris, S. R.; Rawlinson, A. P. *J. Catal.* **1994**, *149*, 254−267.
(25) Mazzone, G.; Rivalta, I.; Russo, N.; Sicilia, E. *Chem. Commun.* **2009**, 1852−1854.
(26) Schunk, S. A.; Lange de Oliveira, A. Acetoxylation of Ethylene. In *Handbook of Heterogeneous Catalysis*; Ertl, G., Knözinger, H., Schüth, F., Weitkamp, J., Eds.; Wiley-VCH: Darmstadt, 2008; Vol. *14*, pp 3464−3479.
(27) Perego, C.; Peratello, S. *Catal. Today* **1999**, *52*, 133−145.
(28) Mears, D. E. *Ind. Eng. Chem. Process Des. Dev.* **1971**, *10*, 541−547.
(29) Weisz, P. B.; Prater, C. D. Interpretation of Measurements in Experimental Catalysis. In *Adv. Catal.*; Frankenburg, W. G., Komarewsky, V. I., Rideal, E. K., Eds.; Academic Press: New York, 1954; Vol. *6*, pp 143−196.
(30) Dekker, F. H. M.; Bliek, A.; Kapteijn, F.; Moulijn, J. A. *Chem. Eng. Sci.* **1995**, *50*, 3573−3580.
(31) Berger, R. J.; Kapteijn, F.; Moulijn, J. A.; Marin, G. B.; De Wilde, J.; Olea, M.; Chen, D.; Holmen, A.; Lietti, L.; Tronconi, E.; Schuurman, Y. *Appl. Catal., A* **2008**, *342*, 3−28.
(32) Drochner, A.; Kampe, P.; Blickhan, N.; Jekewitz, T.; Vogel, H. *Chem. Ing. Tech.* **2011**, *83*, 1667−1680.
(33) van der Linde, S. C.; Nijhuis, T. A.; Dekker, F. H. M.; Kapteijn, F.; Moulijn, J. A. *Appl. Catal., A* **1997**, *151*, 27−57.
(34) Schiesser, W. E. *The Numerical Method of Lines*; Academic Press: San Diego, 1991.
(35) Schiesser, W. E.; Griffiths, G. W. *A Compendium of Partial Differential Equation Models: Method of Lines Analysis with Matlab*; Cambridge University Press: New York, 2009.
(36) Levenberg, K. *Quart. Appl. Math.* **1944**, *2*, 164−168.
(37) Marquardt, D. W. *J. Soc. Ind. Appl. Math.* **1963**, *11*, 431−441.
(38) Hansen, E.; Neurock, M. *J. Phys. Chem. B* **2001**, *105*, 9218−9229.
(39) Haley, R.; Tikhov, M.; Lambert, R. *Catal. Lett.* **2001**, *76*, 125−130.
(40) Bowker, M.; Morgan, C.; Couves, J. *Surf. Sci.* **2004**, *555*, 145−156.
(41) Li, Z.; Gao, F.; Tysoe, W. T. *Surf. Sci.* **2008**, *602*, 416−423.
(42) Kobayashi, H.; Kobayashi, M. *Catal. Rev.: Sci. Eng.* **1974**, *10*, 139−176.
(43) Bennett, C. O. *Catal. Rev.: Sci. Eng.* **1976**, *13*, 121−148.
(44) Kobayashi, M. *Chem. Eng. Sci.* **1982**, *37*, 393−401.
(45) Froment, G. F.; Bischoff, K. B. *Chemical Reactor Analysis and Design*, 2nd ed.; John Wiley & Sons: Toronto, 1990.
(46) Jess, A.; Wasserscheid, P. *Chemical Technology*; Wiley-VCH Verlag: Weinheim, 2013.
(47) Fogler, H. S. *Elements of Chemical Reaction Engineering*, 4th ed.; Pearson Education: Westford, 2006.
(48) Shannon, S. L.; Goodwin, J. G. *Chem. Rev.* **1995**, *95*, 677−695.
(49) Ledesma, C.; Yang, J.; Chen, D.; Holmen, A. *ACS Catal.* **2014**, *4*, 4527−4547.
(50) Gayubo, A. G.; Alonso, A.; Valle, B.; Aguayo, A. T.; Olazar, M.; Bilbao, J. *Chem. Eng. J.* **2011**, *167*, 262−277.
(51) Gatla, S.; Madaan, N.; Radnik, J.; Kalevaru, V. N.; Pohl, M.-M.; Lücke, B.; Martin, A.; Bentrup, U.; Brückner, A. *J. Catal.* **2013**, *297*, 256−263.
(52) Gatla, S.; Madaan, N.; Radnik, J.; Kalevaru, V. N.; Pohl, M.-M.; Lücke, B.; Martin, A.; Brückner, A. *Appl. Catal., A* **2011**, *398*, 104−112.
(53) Schunk, S. A.; Baltes, C.; Sundermann, A. *Catal. Today* **2006**, *117*, 304−310.

DOI: 10.1021/acscatal.6b00646
ACS Catal. 2016, 6, 4621−4629